IAC-10-B4.6B.3

# DESIGN STATUS OF THE DELFI-NEXT NANOSATELLITE PROJECT

J. Bouwmeester
Delft University of Technology, Faculty of Aerospace Engineering, Chair of Space Systems Engineering, Delft, The Netherlands, jasper.bouwmeester@tudelft.nl

G.F. Brouwer
Delft University of Technology, Delft, The Netherlands, g.f.brouwer@tudelft.nl
E.K.A. Gill
Delft University of Technology, Delft, The Netherlands, e.k.a.gill@tudelft.nl
G.L.E. Monna
SystematIC BV, Delft, The Netherlands, b.monna@systematic.nl
J. Rotteveel
ISIS BV, Delft, The Netherlands, j.rotteveel@isispace.nl

## ABSTRACT

Delfi-Next is the second project within the Delfi nanosatellite development program of Delft University of Technology. It will provide students hands-on experience, facilitate technology demonstration for innovative miniaturized space technology from the Dutch space sector and allow advancements in satellite bus performance compared to its predecessor Delfi-$C^3$. This paper will describe the mission and provides insight in the design status and trade-offs of each bus subsystem at September 2010.

A micropropulsion system from TNO, an in-orbit configurable radio from ISIS BV and amorphous silicon solar cells will be demonstrated onboard Delfi-Next.

The electrical power subsystem consists of deployable solar panels, a central power management unit, a battery system and local power regulation units on each printed circuit board. The central power management unit uses redundant maximum power point trackers for each solar panel and distributes the acquired power to a standard system bus on a fixed single supply voltage of 12V, the battery system and a shunt for excessive power.

The communication subsystem consists of two redundant radios transmitting a continuous 1.2-9.6 kbps signal on a 145 MHz carrier frequency, a high data rate S-band transmitter, a receiver and a set of deployable antennae in a turnstile configuration. The downlink is received by a global distributed ground station network consisting of several universities and radio amateurs.

Onboard data handling is performed by a hot redundant onboard computer, which manages and acquires measurement data from local subsystem microcontrollers by means of an $I^2C$ data bus. Because the standard implementation of $I^2C$ lacks failure tolerance it is supplemented with bus buffers on each local system which will isolate malfunctioning nodes from the main bus when necessary.

A custom designed spacecraft structure optimized for accessibility will provide the basis for all physical subsystems which are made compliant to a standardized form factor. The structure complies with the outer dimensions of a triple-unit CubeSat. Passive thermal control based on heat sinks and optical properties of surface materials will keep components and subsystems within the required thermal range.

Attitude determination and control will be performed by a suite of sensors, actuators and processing algorithms to demonstrate active attitude control functionality as a baseline for future Delfi missions.

Future Delfi missions to demonstrate formation flying capabilities are foreseen, potentially within the QB-50 network for thermospheric research or demonstration missions for the OLFAR moon-orbiting radio telescope.

## 1. INTRODUCTION TO THE DELFI-NEXT MISSION

This paper provides an overview of the Delfi-Next mission and its design status at September 2010. The Delfi-Next mission (also written as Delfi-n3Xt) is second in a development line of nanosatellites called the 'Delfi Program' [1] and is successor to the successful Delfi-$C^3$ [2] mission.

The mission statement for Delfi-Next is as follows: *"Delfi-Next shall be a reliable triple-unit CubeSat of TU Delft which implements substantial advances in 1 subsystem with respect to Delfi-$C^3$ and allows technology demonstration of 2 payloads from external partners from 2012 onwards"*.

In the next sections, the Delfi-Next mission is further specified according to the three general objectives of the Delfi program.

### 1.1 Educational objective

The Delfi program shall provide students optimal preparation for careers in space industry. This preparation includes improvement of skills in systems engineering, teamwork, scientific writing, and communication and facilitates hands-on experience with all aspects of the development of a (small) spacecraft.

### 1.2 Technology demonstration objective

Delfi satellites will perform technology demonstration and/or (pre-)qualification of micro-technologies for space applications, emerging from various developments within the Dutch space sector. These technologies can be cooperative developments on the spacecraft bus or experiments which stand alone. In the latter case, these will be referred to as 'payloads' and are explicitly mentioned as mission objectives.

For Delfi-Next, the two payloads onboard are a micro-propulsion system developed by TNO in cooperation with TU Delft and University of Twente called $T^3\mu PS$ and an in-orbit configurable, high-efficient transceiver platform developed by ISIS BV, in cooperation with TU Delft and SystematIC BV called ITRX.

Delfi-Next will carry out an onboard experiment on hydrogenated amorphous silicon solar cells from the micro-electronics institute DIMES from the TU Delft.

Additionally, an experimental very low frequency receiver might be tested as precursor for the OLFAR program [3].

### 1.3 Nanosatellite bus development objective

The Delfi program will advance the nanosatellite platform gradually with the aim to make very small satellites more capable for advanced technology demonstration, scientific or commercial purposes. There is a commonality with the technology demonstration objective, but whereas technology demonstration can stand alone, this objective is to advance the spacecraft bus as a whole on a systematic and consistent matter. In this way, Delfi can create spin-off for the space sector for more advanced scientific or commercial missions. A special emphasis is put on the required developments for formation flying and constellations of nanosatellites. This will enable space applications which have not been feasible before [1].

The mission clearly states that one subsystem should be significantly advanced compared to Delfi-$C^3$. The attitude control system plays an important role in more advanced capabilities for nanosatellites. With full three-axis active control, sun-pointing a solar array could yield more specific power, ground station tracking could be used for higher data-rates, instrument pointing can be used for remote sensing and formation flying is possible if attitude and orbit can be (relatively) controlled. Delfi-$C^3$ is equipped with a passive magnetic attitude control, which is unsuitable for such functionalities. As such, it is decided that Delfi-Next will be significantly advanced in the Attitude Determination and Control Subsystem compared to Delfi-$C^3$.

Next to a significant advancement on the ADCS with respect to Delfi-$C^3$, advancements on other bus subsystems have been identified as feasible and desirable. These are:

- An experimental S-band transmitter, called the STX, which allows for high(er) downlink data rates. Experience with S-band transmitters is considered useful for future mission requiring substantial higher downlink data volumes. Because of its experimental status this S-band transmitter will not perform mission critical functions.
- An electrical power subsystem with onboard energy storage. This will allow for eclipse operation and temporary high power consumption.
- A Single-Point-Of-Failure-free OnBoard Computer (OBC). In Delfi-$C^3$, the backup for operations by the single OBC was a distributed autonomous operation by local microcontrollers. For the more advanced Delfi-Next mission, this solution becomes too complex.
- A robust Command and Data Handling System, with significant less Bit-Error-Rate (BER) and more failure tolerance than on Delfi-$C^3$. A mismatch in clock speeds and failing watch-dogs on Delfi-$C^3$ have lead to an unstable data bus [4].

Chapter 2 to 4 explain the $T^3\mu PS$ and ITRX payloads and the solar cell experiment respectively. Chapters 5 to 9 provide insight in the satellite bus systems and their design status. Finally, chapter 10 provides a conclusion and outlook for the future.

## 2. $T^3\mu PS$ MICRO-PROPULSION PAYLOAD

As briefly mentioned in section 1.3, nanosatellites have a strong potential for novel operational missions when launched in a formation or constellation. This requires relative orbit control for which some form of propulsion is needed. There are however some constraints on nanosatellites which complicates the use of propulsion devices. First of all there are tight technical budgetary constraints such as volume, mass and power. Next to this, nanosatellites are typically secondary or tertiary payloads onboard a launch vehicle. To reduce potential risks to the launch vehicle or primary payload, launch regulations typically forbid the use of highly pressurized tanks and pyrotechnics for nanosatellites. To deal with these constraints TNO, together with the TU Delft and the University of Twente, developed a micropropulsion system based on cold gas generators called the $T^3\mu PS$. Table 1 provides key characteristics of this system onboard Delfi-Next.

| Characteristic | Specification |
|---|---|
| Specific impulse | > 30 s |
| Thrust | 6 – 100 mN<br>(selectable by manufacturing) |
| Propellant mass | *per CGG:* 0.3 g<br>*total:* 2.4 g |
| Total mass | 120 g |
| Dimensions | 90 mm · 90 mm · 35 mm |
| Power consumption (per mode) | *measuring:* 63 mW<br>*thrusting*: 355 mW<br>*igniting:* 10.6 W |

Table 1: Key characteristics of $T^3\mu PS$ on Delfi-Next

Cold Gas Generators (CGGs) store nitrogen in a solidified form. When electro-thermal energy is added, the nitrogen releases in gaseous state and enters in a plenum which will buffer the pressurized gas. A Micro-Electro-Mechanical Systems (MEMS) based valve and nozzle are used to release the gas into space to provide controlled thrust. A schematic overview of this system is presented in Fig. 1 and parts in Fig. 2 and Fig. 3.

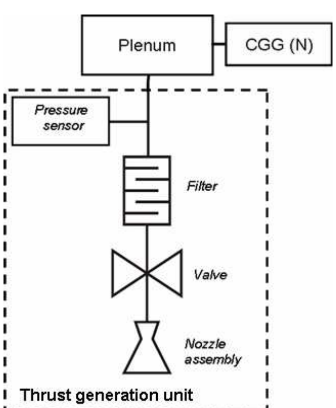


Fig. 1: Schematic overview of $T^3\mu PS$

Delfi-Next will demonstrate this novel micropropulsion system by carrying out the following measurements and experiments:

- Ignition of multiple CGGs.
- Thrusting at various levels with pulse-width-modulated duty cycling.
- Determination of the leakage through continuous plenum pressure measurements during the nominal measurements mode of the micropropulsion system.
- Determination of the thrust by measuring the pressure drop during thrusting onboard and indirectly by minor orbit changes measured on ground by radar tracking stations.
- General housekeeping measurements such as temperature and power consumption.

A functional prototype has been built and tested successfully in a dedicated test setup which is able to measure very low thrust levels. At the time of writing an engineering model is being developed for integration with the Delfi-Next engineering model.

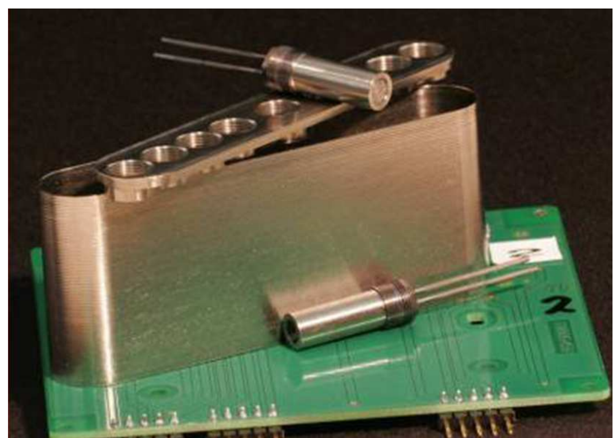

Fig. 2: $T^3\mu PS$ plenum, PCB and CGGs

Fig. 3: $T^3\mu PS$ micro-nozzle prototype

## 3. ITRX IN-ORBIT CONFIGURABLE HIGH-EFFICIENCY TRANSCEIVER

The experimental ISIS Transceiver (ITRX) is an in-orbit configurable radio with high efficiency. ISIS BV, a spin-off company from the Delfi-C$^3$ project, has experience with the development and sales of radios for nanosatellites (Fig. 4).

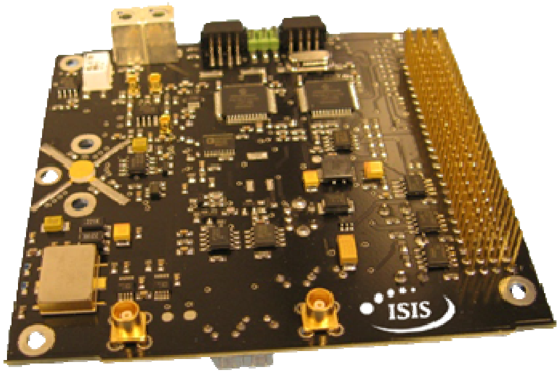


Fig. 4: ISIS' UHF/VHF radio, predecessor of the ITRX.

Each nanosatellite has its unique requirements for a radio. Therefore flexibility of choice for key characteristics such as data rate, modulation, output power and data protocol is desired. At the same time these missions have tight financial budgets. The ITRX aims to tackle this with a standardized radio with easy configurability for the key characteristics. In addition, with the growing interest in CubeSats and other nanosatellites in the world, both from universities and research institutes as from companies and government agencies, it is important to start to think of a more coordinated system of space-ground communication for CubeSats. With the number of CubeSats under development reaching in the hundreds, the available radio spectrum for so many spacecraft is rather limited. A more agile, flexible radio architecture, that has the ability to be (re)configured in orbit, is a first step towards a system that can accommodate all these new spacecraft missions in terms of space-ground communication links. Standardization will bring the cost down while configurability provides the design flexibility demanded by the customers and the community as a whole. As most of this configurability is software defined it is possible to change this in orbit. This will allow the user to adjust the settings of the radio during mission operations to the results of the actual link performance with the ground segment, making the system more tolerant to design flaws or taking advantage of fortunate circumstances allowing for instance higher data rates. Other potential purposes are a gradual stepwise commission phase of the satellite or different radio settings for different satellite modes.

Another issue the ITRX aims to tackle is the very limited available power within nanosatellites. As can be seen in section 5.1, the power consumption of the radio contributes for a significant part to the total power budget of Delfi-Next. The power amplifier in the transmitter section is the most dominant in power consumption. Conventional linear amplifiers have typical efficiencies of about 30%, which means much of the power is wasted as heat. A switching mode power amplifier currently being developed in cooperation between TU Delft, ISIS BV and SystematIC BV can yield efficiency above 80%.

Table 2 provides the key characteristics of the ITRX. Experiments with all in-orbit configurable settings will be carried out during the Delfi-Next mission. The ITRX will also act as backup device for the primary radio as the ITRX can be configured to the same functionality and performance.

| Characteristic | Specification |
|---|---|
| Frequency bands | VHF down, UHF UP |
| Data rate range | 1200 – 9600 bps |
| Modulation options | (A)FSK, BPSK, CW, QPSK, MFSK |
| Protocol options | AX.25, CW, ISIX, DelfiX, etc. |
| Total mass | 90 g |
| Dimensions | 90 mm · 90 mm · 20 mm |
| Power consumption (nominal settings) | *receiver:* 255 mW<br>*transmitter:*: 1580 mW |

Table 2: Key characteristics of the ITRX on Delfi-Next

## 4. AMORPHOUS SILICON SOLAR CELL EXPERIMENT

At the DIMES microelectronics institute of the TU Delft, hydrogenated amorphous silicon (a-Si) solar cells have been produced which will be tested onboard Delfi-Next. These a-Si cells do not have a high efficiency but they are very cost effective and are expected to have a high tolerance against the harsh space environment. The latter will be verified by measuring the temperature, power output and sun irradiation on about 30 small a-Si cells (Fig. 5). The power output will be measured with a 'sweep' through the current-voltage curve with the means of a resistor ladder and precise analog-to-digital converters. The sun irradiance will be measured with a reference photo-diode with well known characteristics.

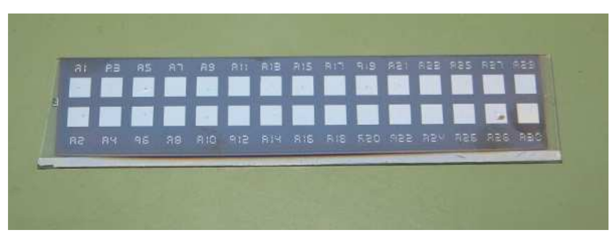

Fig. 5: Batch of a-Si solar cells from DIMES

## 5. ELECTRICAL POWER SUBSYSTEM

The Electrical Power Subsystem (EPS) consists of solar panels, a battery system, a central power conditioning and management system called Global EPS (G-EPS) and local power control. Fig. 6 shows a schematic overview of the distributed EPS of Delfi-Next, with the G-EPS supplying all subsystems with a single supply voltage and local power control switching the subsystems and the providing the required supply voltages to the subsystem components.

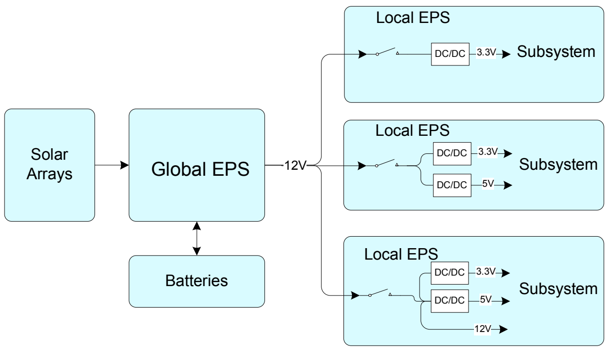


Fig. 6: Schematic overview of the Delfi-Next EPS

### 5.1 Power Budget

The EPS is designed on the required power of the subsystems in the nominal mode (Table 3) in which the satellite will be operating for most of the time (>95%). If the ITRX or STX transmitter is used, the PTRX transmitter will be turned off, yielding an almost power neutral mode transition. Only the ignition of a CGG of the $T^3\mu PS$ microthruster (chapter 2) consumes considerable amount of power (~10 W), but this will only last for about 10 seconds which has an insignificant impact on the energy storage of the batteries. All other satellite modes consume less than the nominal mode.

As the satellite will also be in the nominal mode during eclipse, the average power required from the solar array increases roughly with 50%. Next to that, all conversion losses need to be taken into account.

| Subsystem | Mode | $P_{req}$ [mW] |
|---|---|---|
| $T^3\mu PS$ | measuring | 255 |
| ITRX | receive | 63 |
| SDM | on | 30 |
| G-EPS | on | 50 |
| ADCS | on | 1385 |
| PTRX | transceive | 1845 |
| STX | store | 159 |
| OBC | on | 200 |
| System Bus | on | 255 |
| Mechanisms | off | 0 |
| Total | Nominal | 4242 |

Table 3: Power budget for nominal satellite mode

### 5.2 Solar Panels and Configuration

The solar cells which will be used for Delfi-Next are TEC1D triple junction cells ($GaInP_2/GaAs/Ge$) from TECSTAR. These cells have a decent efficiency of about 23% at a temperature of 28$^o$C and are supplied by Dutch Space as in-kind support. A (deployable) solar panel with dimensions compatible with the long side of the satellite can contain 7 of these cells. Under normal incidence of the sun and a temperature of 28$^o$C, a single panel can deliver 5453 mW of power.

Though Delfi-Next is equipped with a three-axis active attitude control system, the experimental status of this system and its identified risks has led to a requirement that no other subsystem may be critically dependent on the proper functioning of this system. This means that for defining the solar panel configuration, a tumbling satellite about an arbitrary rotation axis must be assumed. To avoid heavy cycling and major dependency on the battery system, it is preferred to have a near omni-directional configuration. This was also the case for Delfi-$C^3$ which had no battery at all and used a tetrahedron configuration as can be seen in Fig. 7. The difference between the minimum and average power can be used to charge the batteries for eclipse operation, limiting battery cycling to the orbital frequency.

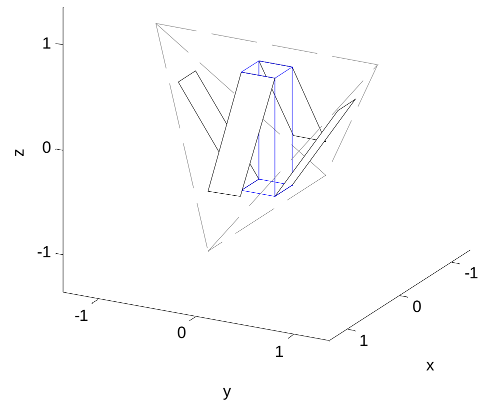


Fig. 7: Tetrahedron solar panel configuration.

Different configurations were analysed on complexity and power. Fig. 9 shows the results of an analysis including shadowing effects for three different configurations: body mounted (only on long sides of the satellite), tetrahedron (similar to Delfi-$C^3$) and a configuration with top-mounted double sided panels optimized to maximize the minimum power (Fig. 8). The power is normalized to the output of a 7-cell array under normal incidence of the sun vector in space at a temperature of 60$^o$ ($n_{7w}$). The required raw power from the power budget is calculated to supply a minimum for the nominal mode and an average including eclipse operation. All expected conversion and storage losses are taken into account.

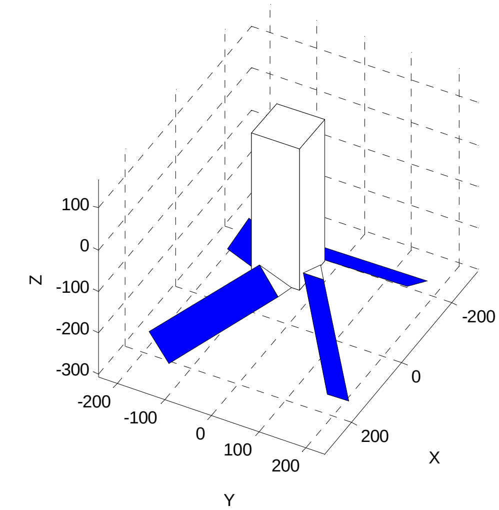

Fig. 8: Top-mounted double sided solar panel configuration

It can be seen from Fig. 9 that a simple body mounted solution will not yield sufficient power by far. The design margins in the power budget are too small too cope with this. A tetrahedron configuration could only be possible if most systems are off in eclipse and the subsystem power is slightly reduced. Although feasible, this will degrade satellite performance and mission return significantly. The configuration with the double-sided solar panels which are attached to the top of the satellite body and deployed under an optimized angle (Fig. 8) yields the highest amount of power and complies well with the required power. Many more possible configurations have been analysed, but most of them yield less power with similar or increased complexity. At the time of writing however, some concerns have arisen from dynamic simulations about potential up-spinning behaviour of this satellite configuration. The final decision on solar panel configuration therefore still has to be taken.

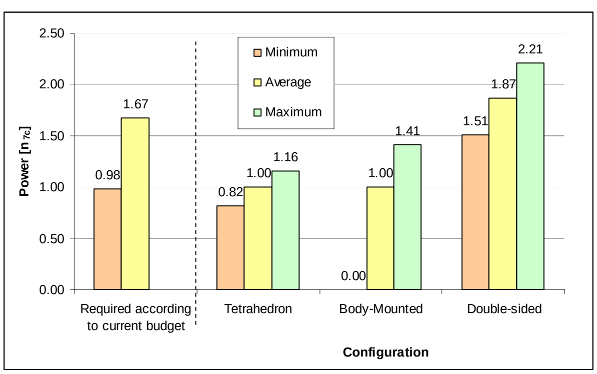

Fig. 9: Normalized required and available solar panel power

5.3 Global EPS Design

Maximum Power Point Trackers (MPPTs) will be used to obtain the electrical energy from the solar panels. These MPPTs provide a safe means to get the most out of the solar arrays in all conditions and performance of the solar cells.

Lithium-ion batteries will be used for energy storage for eclipse operation and temporary events such as the ignition of a CGG of the micro-propulsion payload (see chapter 2). A battery management device will charge a battery, if not fully charged already, when there is sufficient available power and discharge the battery when there is insufficient solar power available.

A regulated single supply voltage of 12 Volt is used for all subsystems. The main reason to go for a single supply voltage is to keep the system bus interfaces to a minimum in order to limit wiring harness and complexity and to standardize the system bus interface. This main power line is protected by the standard system bus interface as explained in section 7.2.

Excess power will be shunted and can be used advantageously in two ways:

1) An operational amplifier in a radio can act as functional shunt, leading to increased downlink margins at times there is excess of power. It is expected that this will increase the overall yield of telemetry received by radio amateurs.

2) A simple resistor acts as shunt and the amount of excess power is measured. The onboard computer can use this knowledge to discretely change to a (subsystem) mode with higher power consumption. This can yield more return from the payload demonstrations and/or onboard experiments.

It is currently under investigation if and which one of these two options will be used.

Fig. 10 provides a schematic overview of the G-EPS. There are four redundant chains in the G-EPS connected to the main system bus which supplies the power to the loads. In case of a single-point-failure in one of the chains, the other remaining chains will still supply 75% of the power on average which will be sufficient for nominal operation during the sunlit part of the orbit.

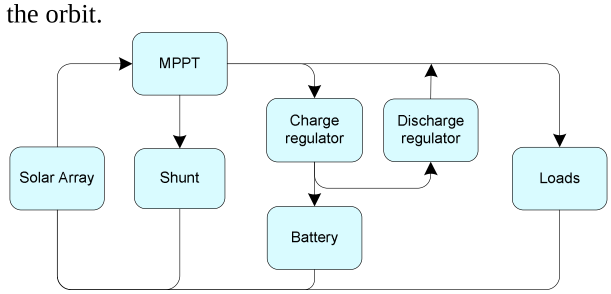

Fig. 10: Schematic functional overview of G-EPS

## 6. COMMUNICATIONS SUBSYSTEM

The communications subsystem (COMMS) of Delfi-Next consists of three radios, a phasing circuit and antennae. Fig. 11 provides an overview of the elements and interfaces of the COMMS. The primary transceiver (PTRX) is the radio used for nominal operations. The second radio is the ITRX which is a payload (chapter 3) but also acts as back-up radio for the PTRX. They both use the same phasing and antenna circuit. The third radio is an S-band transmitter using its own antenna. This radio is experimental and will be used to test an end-to-end link for relatively high data rates.

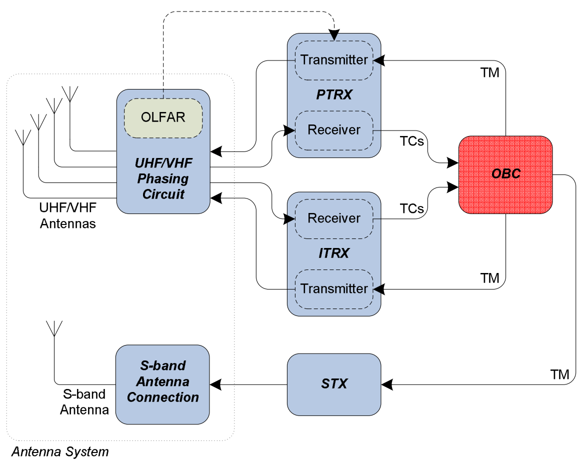


Fig. 11. Overview of the Delfi-Next COMMS

### 6.1 Primary Transceiver

The PTRX is based on the design of the radio of Delfi-C$^3$ and will be slightly improved in performance and reliability.

The PTRX has its uplink frequency in the UHF band at about 435 MHz. The data rate is set at 1200 bps. The uplink is mainly used to tele-command the satellites to change its operational mode, execute experiments or to change operational parameters. The radio is also prepared to be ready for up-linking full software packages for local microcontrollers such as in the OBC and ADCS.

The downlink of the PTRX is in the VHF band at about 145 MHz. The data rate is set at 2400 bps meeting all requirements from payloads, experiments and health monitoring. The transmitter power output of the PTRX is 0.2 W. Including all wiring and antenna losses, the transmitted EIRP output is -14.8 dBW. In a circular orbit of 800 km at a minimum elevation of 10$^o$ a bit-error-rate of $10^{-6}$ is reached with at least 2 dB ground station antennae gain. This will allow many radio amateurs to participate in the distributed data reception with simple antennae, while still providing a significant improvement over Delfi-C$^3$ which has a data rate of 1200 bps.

The PTRX is further complimented with a linear transponder (UHF up, VHF down) as a return of favour to radio amateurs and might also be equipped with an experimental OLFAR transponder for very low frequencies, which is briefly explained in chapter 10.

### 6.2 S-band Transmitter

The experimental S-band transmitter will be used to develop nanosatellite technology which can yield much higher data rates and to determine how a practical link can be improved to achieve the highest data downlink volumes possible. To make this link more useful than just experimental, all data sent to the PTRX is also stored on the STX. The STX can be requested to resent the packets of a specific time window to obtain missing packets from times in which there was no ground station able to receive the telemetry. The reason this data buffer is located at the STX rather than the OBC is because the STX can have higher data rates than is possible over the I$^2$C data bus at this moment.

The architecture of the STX is kept simple; the key elements are already available as COTS components. As the maximum data rate which can be achieved with a closed link budget is linearly dependent on the amount of output power and the total amount of power to the STX is limited, the efficiency of the power amplifier is a significant factor.

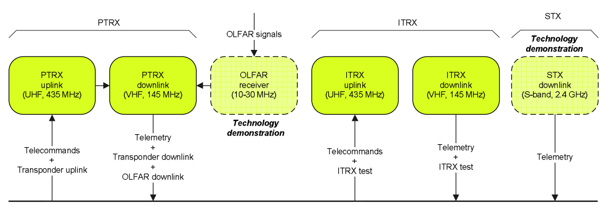


Fig. 12: Overview of Delfi-Next radios and there in- and outputs

### 6.3 Antenna System

The antenna system contains a set of four VHF antennae in a turnstile configuration. As the uplink frequency has a wavelength of approximately one third of the downlink frequency, the VHF antennae can be used for UHF reception as well. For this, an advanced phasing circuit (Fig. 13) is designed which puts the output of the four antennae in phase, isolates the transmitter from the receiver effectively and connects to both PTRX and ITRX. The VHF/UHF antennae (Fig. 14) are custom designed in Modular Antenna Boxes (MABs), which is further explained in section 8.2.

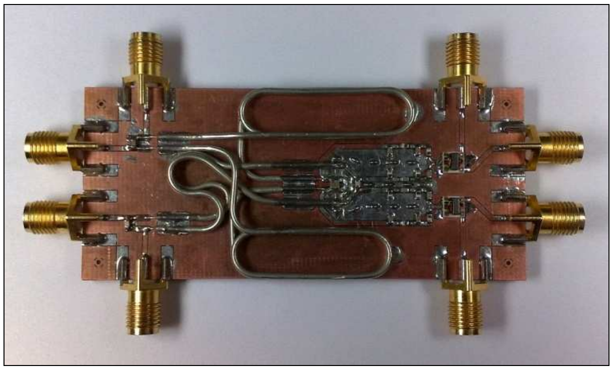

Fig. 13: Advanced UHF/VHF phasing circuit prototype

The S-band transmitter will be connected to a simple patch antenna (Fig. 14) which doesn't require any phasing or isolation network.

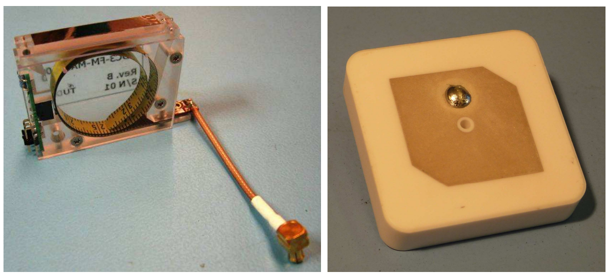

Fig. 14: MABs for UHF/VHF (left) and patch-antenna for S-band (right)

6.4 Ground Station Network

The distributed ground station network consists of a ground station in Delft which is used for telemetry reception and tele-commanding of the satellite complimented with hundreds of radio amateur ground stations around the world for telemetry reception. The network can further be complimented with the GENSO university network of ground stations, providing up- and downlink capabilities at various locations around the world.

For telemetry reception, a steerable antenna, a VHF receiver and a PC with soundcard is required. A telemetry software client which is developed at TU Delft can demodulate the BPSK baseband signal entering the soundcard and decode the telemetry packets. The content of the packets will be displayed onscreen to the radio amateur and the packets will be sent in raw format to the central data server in Delft over the internet.

The central data server in Delft will store all received telemetry data-packets and will perform filtering of erroneous data and processing of the raw data into physical values. An online user interface is being developed to present telemetry data in an easy-to-use manner for satellite operators and telemetry analysts at the project partners. All of this will take place near real-time.

## 7. COMMAND AND DATA HANDLING SUBSYSTEM

The Command and Data Handling Subsystem (CDHS) consists of the redundant onboard computer, local microcontrollers, software and the onboard data bus. As the data bus and electrical power bus have significant interaction, they are combined as the standard system bus (SSB) and placed under the CDHS branch.

7.1 Onboard Computer

The microcontroller for the Onboard Computer (OBC) chosen for Delfi-Next is the MSP-430F1611 of Texas Instruments. This microcontroller has flight heritage on Delfi-$C^3$ and many other nanosatellites [5]. In a radiation test carried out by a TU Delft student in cooperation with EPFL and PSI in Switzerland, this microcontroller performed well up to a total ionization dose of 37 kRad without major errors or catastrophic failure. This will yield more than five years of lifetime in Low Earth Orbit. The heritage, results of the radiation test and the very low power consumption has led to the selection of this microcontroller.

To provide unique frame identification to telemetry packets and correlate the measurements to time, the OBC is equipped with a Real Time Clock (RTC). The selected RTC is more stable in temperature than an internal clock of the microcontroller, and might be supplied with a very small battery power source for keeping time prior and during launch and in case of temporary satellite brownouts.

Two additional functionalities are still optional: software upload capability and local data storage. The OBC still needs to be prototyped at the time of writing, and as such the extra non-mission critical functionalities will only be added after a working and tested prototype has been built.

In Delfi-$C^3$, a distributed back-up mode, in which a few local microcontrollers performed degraded mission operations in an autonomous manner, was designed for the case of an OBC or data bus failure. This back-up system was however very complex and has cost much development time which would have better be spent on testing and improving the reliability of the nominal mode. For Delfi-Next, the OBC will therefore be fully redundant to increase the overall reliability of the satellite in a simple manner. The data bus will be protected against failures as explained in the next section. In case the primary OBC is silent on the bus for a while, the secondary OBC will take over the control. Both OBCs will be placed on the same PCB, but with a fully separated circuit. Table 4 provides the key characteristics of an OBC.

| Characteristic | Specification |
|---|---|
| Microcontroller | MSP-430F1611 |
| Clock speed | 8 MHz |
| Total mass | 60 g |
| Dimensions | 90 mm · 90 mm · 15 mm |
| Power consumption | *single OBC :* 100 mW |

Table 4: Key characteristics of the OBC on Delfi-Next

## 7.2 Standard System Bus

For Delfi-Next, a Standard System Bus (SSB) has been developed which connects all subsystems electrically. As designing for reliability becomes more complex with multiple interfaces, a lean approach has been chosen. The power interface only consists of a 12V supply line, as discussed in section 5.3, and a ground.

The data bus chosen for Delfi-Next is the Inter-Integrated-Circuits ($I^2C$) data protocol, which is a two wire serial interface also used in Delfi-$C^3$. Many data busses have been compared, with its closest competitor being the CAN bus which is also used in some nanosatellites [5]. The reasons to choose $I^2C$ over CAN, despite the fact that CAN has better inherent reliability, are:

- $I^2C$ consumes about 10 times less power than CAN in a comparable set-up.
- There are many peripherals with an embedded $I^2C$ controller, such as microcontrollers, RTCs, ADCs, I/O ports, etcetera.
- There is flight heritage and experience with Delfi-$C^3$.

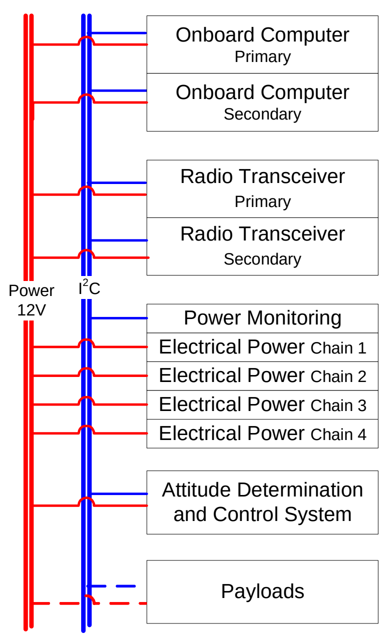


Fig. 15: Schematic overview of standard system bus and the connected subsystems.

In the Delfi-$C^3$ project, it has been discovered that microcontrollers can have failure modes in which they pull one or both of the $I^2C$ lines down indefinitely [4]. The four functional wires of the SSB (12V, ground $I^2C$ clock & $I^2C$ data bus) are simply doubled for redundancy in case of a wire break. Fig. 15 provides a schematic overview of the SSB on Delfi-Next.

There are many $I^2C$ bus buffers available which deal with this problem, including watch-dog circuitry which isolates the node if it occupies the bus for too long. A latch-up free solution is chosen for Delfi-Next, which function is referred to as '$I^2C$ protector'.

Most subsystems need to be able to be switched on or off according to the operational mode and available power. Next to this, as a short circuit can take down the main power bus, a form of over current protection should be placed on each subsystems. There are some integrated circuits which can control a power switch on $I^2C$ command or by detection of over-current. Additionally, these can measure the current for nominal housekeeping data. This functional block is referred to as 'power monitor & controller'.

The $I^2C$ protector, a power switch and the power monitor and controller are put in a SSB protection circuit which is placed on each subsystem and payload closed to the connector(s) as can be seen in Fig. 16. The system bus is a redundant flex-rigid cable with the four functional wires, which connects to a redundant pair of connectors on each physical PCB.

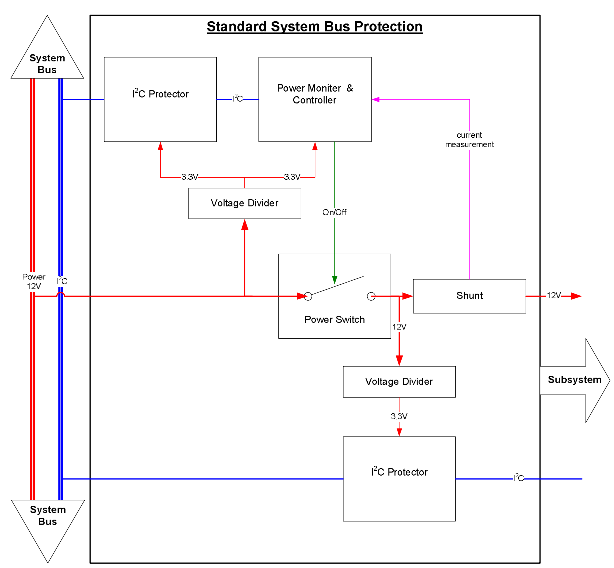


Fig. 16: Functional overview of the standard system bus protection circuit.

## 8. STRUCTURAL SUBSYSTEMS, DEPLOYMENT MECHANISMS AND THERMAL CONTROL

The structural subsystem consists of an outer structure and inner structure and has strong interfaces with the deployment mechanisms and passive thermal control.

### 8.1 Structural Subsystem

The structural subsystem (STS) has an outer structure which complies with the standard triple-unit CubeSat dimensions. This was one of the main constraints originating from the mission statement (see chapter 1). Several options for the structure has been considered, with an outer structure with two detachable L-shaped side panels, a CNC-milled top and bottom panel (TOP & BOP), an intermediate panel and a stack of Printed Circuit Boards (PCBs) held in place with rods and tubes as final result. Table X provides an overview of the key characteristics of the STS.

| Characteristic | Specification |
|---|---|
| Outer dimensions | 100.0 · 100.0 · 340.5 $mm^3$ |
| PCB dimensions | 90.0 mm · 90.0 mm |
| Material | Aluminium |
| Total mass | 651 g |

Table 5: Key characteristics of the STS on Delfi-Next

Detachable L-shaped side panels are chosen to provide easy access and mounting, while keeping manufacturing relatively simple. An intermediate panel and midplane standoffs connected to the rods provides additional stiffness. As antennae, the SDM experiment and sun sensors protrude the outer structure on the bottom and top and they should contain standoffs for the launch deployment adapter, the TOP & BOP are CNC-milled.

The inner structure consists of a stack of PCBs on rods, which are distanced with tubes. Fig. 17 gives an example of Delfi-$C^3$ in which this system was already used, as well as in many other CubeSats. However, as the standard system bus for Delfi-Next deviates very much from the PC/104 standard used in the majority of CubeSat systems, a slightly different PCB lay-out is chosen which provides more space for electrical circuits on the PCB and is fully symmetric.

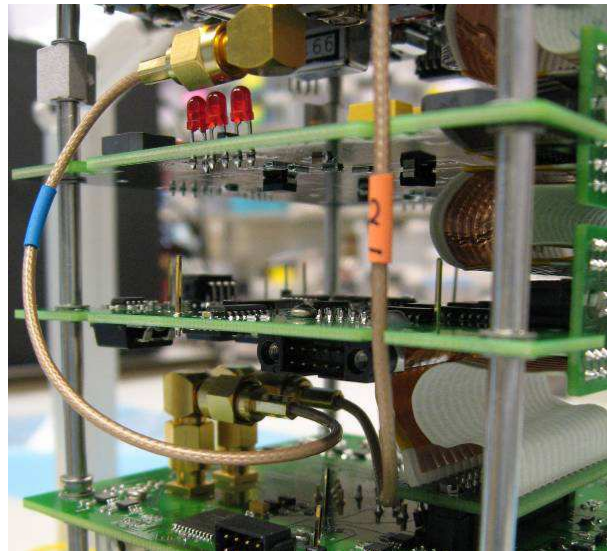

Fig. 17: Example of rod system of Delfi-$C^3$

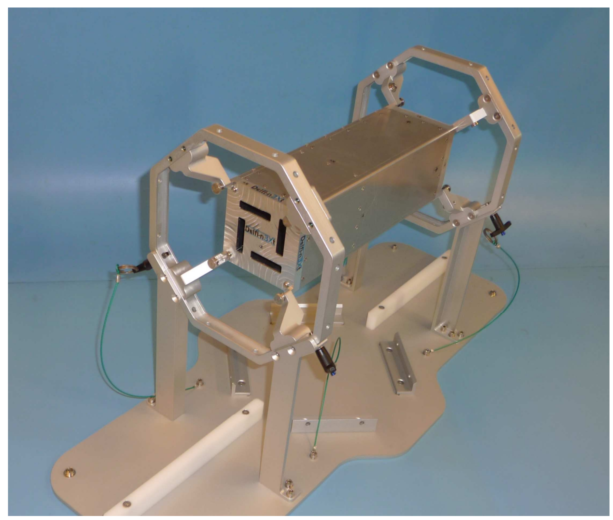

Fig. 18: Delfi-Next prototype of outer structure in integration jig.

### 8.2 Deployment Mechanisms

Delfi-Next has deployment mechanisms for the solar panels and VHF/UHF antennae. The system is based on Delfi-$C^3$ heritage, which had 12 of these systems of which all were deployed successfully. The concept is rather simple; a restraining wire holds the solar panel or lid of the Modular Antenna Boxes (MABs) in place and is burned by a redundant low power thermal knife. The antenna inside the MABs (Fig. 14) is made of measuring tape, which shows a springiness behaviour when the lid is opened. After deployment, the lid with optical tape on top closes again to prevent high local thermal influx. The solar panels have a hinge with deployments stops and two springs, which keep the solar panel at the desired angle once deployed. For all deployment mechanisms a power of 1.92 W is required for approximately 12 seconds.

### 8.3 Thermal Control

The thermal control of Delfi-Next is aimed to be passive. With heat radiators, heat sinks and thermal isolation inside the satellite and optical tapes on the outer structure of the satellite, all systems should be kept within their nominal operating temperatures.

A preliminary thermal finite element analysis has been performed providing insight in the thermal issues which needs to be dealt with. However, as the satellite orbit and the solar panel configuration have a significant influence on the thermal housekeeping, a design will not be worked out yet before these are fixed.

The items which have been identified as critical for cold temperatures are the (dis-)charging of the battery system and the ignition of a CGG of the $T^3\mu$PS micropropulsion payload which both operate best above 10 $^oC$. In the current non-optimized design they can reach temperatures of about - 15 $^oC$ in eclipse and 35 $^oC$ during the sunlit part of the orbit. As ignition for the $T^3\mu$PS can take place in a large time window, a control loop which waits for the temperature to reach the threshold value can deal with this problem. For the batteries, which are used in eclipse by default, a passive solution will be sought which elevates the entire temperature range above the lower threshold. Active heating is not preferred as the thermal capacity of the battery system is high and would therefore require significant amount of energy and this would yield a risky circular control loop; keeping the batteries on temperature would require energy from the batteries.

The hot temperatures inside the temperature are not problematic as the passive components stay below 40$^o$C. Thermal hotspots can be found in electrical components which have relatively high power losses, such as operational amplifiers and the reaction wheel. With a thermal radiator or good conduction to a heat sink, these thermal hotspots can effectively be dealt with in a simple manner. Only the solar panels, which are conductively decoupled from the satellite body, can reach high temperatures of about 90$^o$C which negatively affects their efficiency. This is however taken into account in the power budget.

## 9. ATTITUDE DETERMINATION AND CONTROL SUSBSYTEM

The Attitude Determination and Control Subsystem (ADCS) consists of a set of attitude sensors, actuators and a microcontroller with the control algorithms [7]. The system has an experimental status and the design is aimed to demonstrate the following capabilities:

- Detumbling of the satellite from its deployment from the adaptor on the launch vehicle from initial rates up to 10 $^o$/s to less than 0.2 $^o$/s.
- Three-axis stabilization and pointing the satellite with an accuracy of 3$^o$ to several fixed vectors: sun vector, the velocity vector, the magnetic field line and nadir.
- Slewing manoeuvre for ground station tracking of the S-band antenna with 5$^o$ accuracy.

### 9.1 ADCS Determination

The sensor suite of the ADCS of Delfi-Next consists of (coarse) sun sensors, magnetometers and gyros.

For sun vector acquisition at least six photodiodes are used, potentially complimented with fine micro sun sensors which are being developed by TNO. The photodiodes can determine the incidence angle of the sun with respect to the normal of their plane with about 2$^o$ accuracy when calibrated. This will however only provide knowledge about the cone on which the sun vector may lie. Furthermore there is significant Earth albedo in Low Earth Orbit (LEO) which can yield an offset of about 30$^o$. A smart algorithm, combining the measurements of all photodiodes and taking albedo into account is currently being developed to deal with this in an effective manner.

For measuring the magnetic field, the HMC5843 three-axis digital compass of Honeywell is chosen. This micro sensor provides accuracy for measuring the magnetic field in LEO of about 3$^o$, if bias can be filtered out successfully. As the magnetometer will be placed inside the satellite, care should be taken that no other parts in the satellite have a residual magnetic field which cannot be filtered out in the determination algorithm.

Sun sensors will not work in the eclipse of the orbit, which is approximately 35 minutes in a typical circular LEO. Therefore the sensor suite is complemented with the L3G4200DH of ST micro-electronics which is digital package of three-axis MEMS gyros with accuracy of about 0.01$^o$/s, yielding a maximum offset of about 20 $^o$ at the end of the eclipse for the gyros alone.

All measurements from the sensor suite will be processed on an X-MEGA A1 microcontroller from Texas Instruments. This controller has a large amount of in- and outputs which are more suitable than those of the MSP-430F1611 which is used as default microcontroller onboard Delfi-Next (section 7.1). Furthermore it provides a computational power of 32 MIPS compared to the maximum of 8 MIPS of the MSP-430F1611.

The determination filter which will be used is an unscented Kalman filter. This filter is currently tested in a dynamic system simulator with the selected sensors, but it remains to be programmed for a microcontroller to provide a definitive answer on the suitability of this type of filter within the constraints of the chosen ADCS hardware.

9.2 ADCS Control

The actuator suite of the ADCS consists of three magnetorquers and three reaction wheels, both developed at the TU Delft.

The reaction wheels provide direct control over each of the principle axes of the satellite. They are designed to be able to counteract the highest possible disturbance torque and store the equivalent momentum produced in half an orbit. The rationale behind this requirement is that in the worst case scenario disturbance torques might accumulate for half an orbit around the magnetic field line where the magnetorquers will not be able to dump momentum. The key characteristics of the reaction wheels are shown in Table 6.

| Characteristic | Specification |
|---|---|
| Maximum torque | $9.0 \cdot 10^{-5}$ mN·m |
| Momentum storage | $1.5 \cdot 10^{-3}$ N·m·s |
| Peak Power | 0.135 W per RW |
| Total mass (3 reaction wheels + bracket) | 104 g |

Table 6: Key characteristics of the reaction wheels

The reaction wheel is designed in a pragmatic manner. The basis is a brushless direct current commercial off-the-shelf motor from Faulhaber with integrated speed controller. The lubricant is replaced by the manufacturer to withstand the space environment. A CNC-milled flywheel of bronze is placed on the axis of the motor to provide the required momentum storage. The flywheel is optimized for a high mass moment of inertia per unit weight.

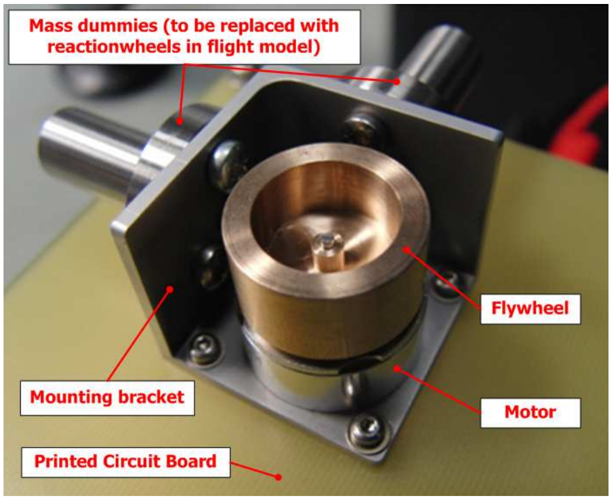


Fig. 19: Prototype of orthogonal reaction wheel assembly

A prototype has already been built (Fig. 19) and tested in two vibration test facilities. The first tests were performed on a vibration shaker at the TU Delft's faculty of mechanical, maritime and materials engineering. The reaction wheels withstood the random noise testing without any signs of degradation, but due to limitations of the shaker, the test levels were slightly insufficient to represent the major launch vehicles. A second test was performed at NLR in a representative structural dummy which was placed within the ISIPOD from ISIS BV. The test levels were very severe, being an envelope of multiple launch vehicle levels including some very harsh ones. This test resulted in the disintegration of one of the reaction wheels and a failure of another. Currently, some redesign is performed on the reaction wheels to strengthen the construction and pitch its first eigen-frequency which is considered to be too low in the current design. For the next test, acceptance levels of some of the dominant CubeSat launchers will be applied.

The magnetorquers are designed to dump momentum of the spacecraft and the reaction wheels. It is a simple electric coil, which gives a magnetic moment when electric current flows through it. Together with the Earth magnetic field, a torque can be created in the axes orthogonal to the magnetic field line.

A prototype has been built of an aircoil. This type of electric coil doesn't have a residual dipole when there is there is no current anymore. This eases the determination of the magnetic field with an onboard magnetometer.

The control of the actuators will be either a PID controller or a more sophisticated LQR method. Both of these controllers have been simulated successfully, but remain to be programmed in the X-MEGA processor.

## 10. CONCLUSION AND FUTURE OUTLOOK

Delfi-Next is an innovative nanosatellite with triple-unit CubeSat dimensions. On each subsystem, advancements are made compared to its predecessor Delfi-$C^3$. The most striking advancement is the active attitude control system which will enable much more functionality for future Delfi nanosatellites. The design status of the subsystems varies at the time of writing from system to system. Preliminary design for all subsystems has been finished. For the electric power subsystem however, some of the preliminary design is currently being reconsidered due to some issues with the solar panel configuration. Some systems are currently well advanced, such as the structural system which already a representative prototype. Most subsystems have been bread-boarded partially on component or section level. Within the ESA standard specification of project phases, the project overall can be placed in the middle of phase C, or detailed definition phase.

For Delfi nanosatellites beyond Delfi, a few opportunities have been identified. One of these opportunities is the QB-50 network of CubeSats [8] for thermospheric research. TU Delft has the intention to fly two similar Delfi satellites within this network, to demonstrate formation flying capability and enhance the scientific return from the QB-50 mission by fixing the spatial distance and/or perform a controlled re-entry in the atmosphere. The results of the experimental attitude determination and control subsystem and the micropropulsion system onboard Delfi-Next will be of great importance for such a mission.

The Orbiting Low Frequency ARray (OLFAR) is a moon constellation of CubeSats which act as a giant distributed radio telescope for extremely low frequencies [3]. It is an extension of the existing Low Frequency Array (LOFAR) within the Netherlands and neighbouring countries. Frequencies below 30 MHz from deep space are reflected by the ionosphere and radio sources from Earth yield significant noise. In space, these issues are less severe and the moon acts as a shield against noise from Earth at the far side of the moon. Delfi-Next may already demonstrate some receiver technology for this mission, but it can be expected that future Delfi nanosatellites will demonstrate other more advanced technologies for this missions as well.

Delfi-Next is being developed on the foundations of the successful Delfi-$C^3$ mission. It is one step further in maturity of nanosatellites, demonstrating all the functionality (but not the performance) as can be found in larger spacecraft. It fills in the missing link towards advanced missions with formations and/or constellations of nanosatellites.

## ACKNOWLEDGEMENT

The authors would like to thank all Delfi-Next team members, project partners, sponsors and financial partners who have all significantly contributed to the Delfi mission and therefore indirectly to the content of this paper. Their individual names can be found on the Delfi website www.delfispace.nl.

## REFERENCES

1. J. Bouwmeester, E.K.A. Gill, C.J.M. Verhoeven, *Advancing Nanosatellite Platforms: The Delfi Program*, Proceedings of the International Astronautical Congress 2008, Glasgow, Scotland, 2008.
2. R.J. Hamann, J. Bouwmeester, G.F. Brouwer, *Delfi-C3 Preliminary Mission Results*, Proceedings of the 23rd annual AIAA/USU Conference on Small Satellites, Logan, USA, 2009.
3. S.J. Engelen, C.J.M. Verhoeven, M. Benthum, *OLFAR, A Radio Telescope Based on Nanosatellites in Moon Orbit*, Proceedings of the 24th annual AIAA/USU Conference on Small Satellites, Logan, USA, 2010.
4. N.E. Cornejo, J. Bouwmeester, G.N. Gaydadjiev, *Implementation of a Reliable Data Bus for the Delfi Program*, Proceedings of the 7th IAA Symposium on Small Satellites for Earth Observation, Berlin, Germany, 2009.
5. J. Bouwmeester, J. Guo, *Survey of Worldwide Pico- and Nanosatellite Missions, Distributions and Subsystem Technology*, Acta Astronautica Vol. 67, Netherlands, 2010.
6. S.Y. Go, J. Bouwmeester, G.F. Brouwer, *Optimized Three-unit CubeSat Structure for Delfi-n3Xt*, Proceedings of the 59th International Astronautical Congress, Glasgow, Scotland.
7. S. Brak, R. Amini, P. Massioni, *Student Nanosatellite Development : From Passive Stabalization to Three-Axis Active Attitude Control*, Proceedings of 32nd Annual AAS Guidance and Control Conference, Breckenridge, USA, 2009.
8. E.K.A. Gill et. al., *Formation Flying to Enhance the QB-50 Space Network*, Proceedings of the 4 Symposium, Funchal, Portugal, 2010.